

Determination of equivalent mechanical parameters for stone-column improved soil using finite-element modelling

Détermination de paramètres mécaniques équivalents pour un sol amélioré par des colonnes ballastées au moyen d'éléments finis

N. Lambert

Tractebel Engineering, Brussels, Belgium

P. Debauche

Tractebel Engineering, Brussels, Belgium

ABSTRACT: To reduce the global stiffness of a large building, soil improvement is considered instead of deep foundations. Settlements and differential settlements are analysed with a 3D finite element code. Due to the dimensions of the building, it is not possible to model each individual stone column. However, equivalent mechanical parameters based on common empirical formulas prove to be too pessimistic. Equivalent geomechanical parameters are therefore determined from auxiliary limited models where individual stone columns are considered. The soil is modelled with the advanced behaviour law 'Hardening soil with small strain stiffness' available in Plaxis.

A large-scale load test with back-analysis is foreseen to validate the design.

RÉSUMÉ: Afin de diminuer la raideur globale d'un bâtiment de grande taille, l'option de l'amélioration de sol est envisagée au lieu de fondations profondes. Les tassements totaux et différentiels sont analysés au moyen d'un code aux éléments finis 3D. Vu les dimensions du bâtiment, il n'est pas possible de modéliser des colonnes ballastées individuellement. Les paramètres mécaniques équivalents basés sur les formules empiriques usuelles s'avèrent trop pessimistes. Des paramètres géomécaniques équivalents sont déterminés à partir de modèles auxiliaires incluant explicitement des colonnes ballastées. Le sol est modélisé au moyen d'une loi de comportement hyperbolique avec écrouissage et prise en compte de la raideur en petites déformations, disponible dans Plaxis.

Pour valider le design, un essai de chargement à grande échelle avec analyse régressive, est prévu.

Keywords: Soil improvement; Stone columns; Finite elements

1 INTRODUCTION

A new large-dimension storage building must be constructed on a soft soil not allowing shallow foundations: bearing capacities are problematic

and settlement criteria are not fulfilled. To limit the global stiffness of the structure in case of earthquake, shallow foundations on improved soil are considered as alternative to piles.

2 STORAGE BUILDING

The building's footprint is 87 x 31 m². It rests on a 1.5m-thick raft. Wall thickness range from 0.7 to 1.0 m. Below the walls, the loads are ranging between 190 and 700 kN/m. Inside the building, variable loads vary between 10 and 125 kPa.

3 GEOTECHNICAL CONTEXT

The subsoil is composed of silty to clayey alluvions resting on gravelly alluvions. Palaeozoic bed-

rock is composed of shale, below the southeastern part of the site, and calcareous rock below the northwestern part. The top of the shale bedrock is weathered on the upper 20 to 50 cm. The stratigraphy and the main field test results are summarised in Table 1 where q_c (MPa) is the tip resistance of the Cone Penetration Test, and p_l (MPa), E_M (MPa) are respectively the limit pressure and Menard modulus of the Menard PressureMeter Test. The numbers between brackets are the values used in the correlations.

Table 1. Stratigraphy and main field test results

Layer	Depth (m)	CPT – q_c (MPa)	PMT – p_l (MPa)	PMT – E_M (MPa)
Silty/clayey alluvions (NW)	0...10	1	1	5
Silty/clayey alluvions (SE)	0...10	5...25 (15)	1...3 (2)	5...10 (8)
Gravelly alluvions	10...14	10...35 (25)	2...6 (4)	25...65 (40)
Bedrock (NW)	14...	>50 (50)	>8 (8)	>200 (200)
Bedrock (SE) – weathered	14...20	>50 (50)	2...8 (5)	50...200 (100)
Bedrock (SE) – sound	20...	>50 (50)	>8 (8)	>200 (200)

4 STONE COLUMN LAYOUT

The soil improvement consists of around 1,500 stone columns with a nominal diameter of 80 cm installed according to a triangular pattern down to the gravel layer (≈ 10 m long). The axis-to-axis distance is 1.90 m. An extra-band of 10 m in X & Y directions provides with confinement.

5 MODELLING

In Plaxis 3D, soils are modelled with volume elements and structures with plate elements. Two of the behaviour laws available in Plaxis are used:

- A linear elastic – perfectly plastic law (Figure 1) with a Mohr-Coulomb failure criterion (Figure 2);
- An hyperbolic law with hardening and small-strain stiffness (HSSsmall).

In HSSsmall law (Figure 3), the stiffness is stress-dependent. Permanent strains develop from the beginning of primary loading. Only reversible strains develop in unloading/reloading. The stress-dependant stiffness parameters are related to a reference pressure:

$$\frac{E_{oed}^{ref}}{E_{oed}} = \left(\frac{p_{ref} + c' \cdot \cot \phi'}{-\sigma'_1 + c' \cdot \cot \phi'} \right)^m \quad (1)$$

$$\frac{E_{50}^{ref}}{E_{50}} = \frac{E_{ur}^{ref}}{E_{ur}} = \left(\frac{p_{ref} + c' \cdot \cot \phi'}{-\sigma'_3 + c' \cdot \cot \phi'} \right)^m \quad (2)$$

Where $E_{oed}^{(ref)}$, $E_{50}^{(ref)}$ and $E_{ur}^{(ref)}$ (kPa) are respectively the oedometer compression modulus, the secant modulus at 50% of the failure deviator and the unloading/reloading secant modulus; the superscript (*ref*) refers to the reference pressure p_{ref} (kPa). The exponent 'm' is related to the nature of the soil (usually 0.5 to 1.0).

The small-strain behaviour is described by a reduction curve providing with the relationship

between the shear modulus G (kPa) and the angular strain (or distortion) γ (-) (Figure 4).

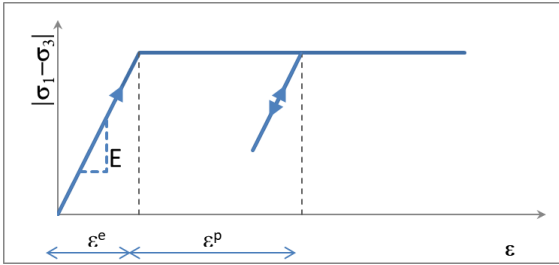


Figure 1 – Strain-stress in 'Mohr-Coulomb' law

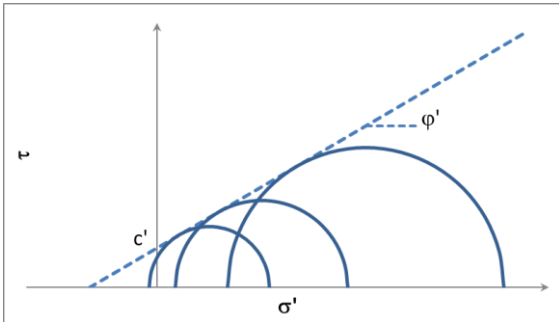


Figure 2 – Mohr-Coulomb failure criterion

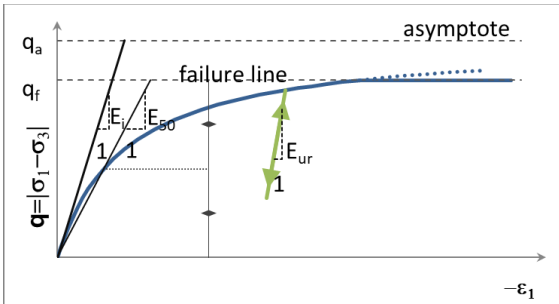


Figure 3 – Hyperbolic strain/stress relationship

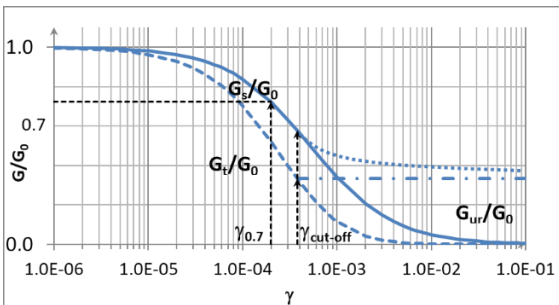


Figure 4 – Small-strain behaviour – example of reduction curve

According to Hardin-Drnevich:

$$\frac{G_s}{G_0} = \frac{1}{1+a \left| \frac{\gamma}{\gamma_{0.7}} \right|} \quad (3)$$

$$\frac{G_t}{G_0} = \frac{1}{\left(1+a \left| \frac{\gamma}{\gamma_{0.7}} \right| \right)^2} \quad (4)$$

Where G_s , G_t and G_0 (kPa) are respectively the secant, tangent and small-deformation shear moduli. The parameter a (-) is equal to 0.385 and $\gamma_{0.7}$ is the distortion for $G_s \approx 0.7 G_0$ (kPa). For $\gamma \geq \gamma_{\text{cut-off}}$, $G_t = G_{ur}$, with

$$G_{ur} = \frac{E_{ur}}{2(1+\nu_{ur})} \quad (5)$$

Where ν_{ur} (-) is the unloading/reloading Poisson coefficient, by default equal to 0.2 in Plaxis.

6 DESIGN PARAMETERS

6.1 Correlations

The oedometer modulus is deduced from Table 1, from the Ménard modulus or, from the CPT tip resistance q_c (Lunne, 1997):

$$\begin{cases} E_{oed} = 4 \cdot q_c & q_c < 10 \text{ MPa} \\ E_{oed} = 2 \cdot q_c + 20 \text{ MPa} & \text{for } 10 \leq q_c < 50 \text{ MPa} \\ E_{oed} = 120 \text{ MPa} & q_c \geq 50 \text{ MPa} \end{cases} \quad (6)$$

For the HSSmall law, the ratios between the moduli are defined by (Brinkgreve, 2014):

$$E_{50}^{ref} = \begin{cases} E_{oed}^{ref} & \text{for sands} \\ 2 \cdot E_{oed}^{ref} & \text{for clays} \end{cases} \quad (7)$$

$$E_{ur}^{ref} = \begin{cases} 3 \cdot E_{50}^{ref} & \text{for sands} \\ 5 \cdot E_{50}^{ref} & \text{for clays} \end{cases} \quad (8)$$

The reference small-deformation modulus is deduced from the large-strain moduli (Brinkgreve, 2017):

$$G_0 = k \times \frac{E_0}{E_{ur}} \cdot \frac{E_{50}}{2 \times (1 + \nu_{ur})} \quad (9)$$

Where k (-) is the factor 3 for sands, 5 for clays as defined in equation (8).

The ratio between E_0 and E_{ur} is given on Figure 5 (Brinkgreve, 2017).

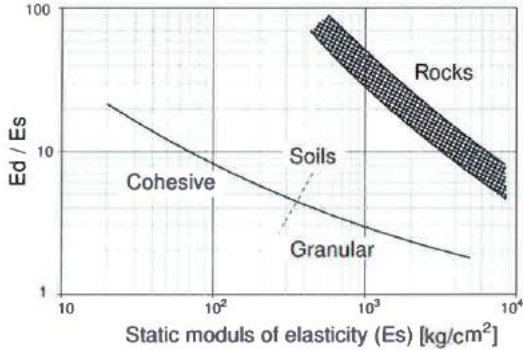


Figure 5 – Relation between dynamic ($E_d = E_0$) and static soil stiffness ($E_s \approx E_{ur}$) after Alpan (1970)

The parameter $\gamma_{0.7}$ is estimated by the following formula (Brinkgreve, 2017):

$$\gamma_{0.7} \approx \frac{1}{9 \cdot G_0} [2c'(1 + \cos 2\phi') - \sigma'_{v0}(1 + K_0) \sin 2\phi'] \quad (10)$$

6.2 Bedrock

To limit the influence of the thickness of the bedrock on the model, this layer is modelled with the HSSmall law (Table 2).

6.3 Soft soil

The gravelly alluvions are modelled with the ‘Mohr-Coulomb’ law: the layer is relatively stiff and has a limited thickness, so (differential) settlements will be limited. The silty/clayey alluvions surrounding the building are modelled with the ‘Mohr-Coulomb’ law (Table 3).

6.4 Improved soil

The extent of the improved soil area being large, modelling individual stone columns below the

building is not an option. Equivalent soil properties can be defined according to several options.

6.4.1 Empirical approach

The equivalent soil parameters are determined with empirical formulas. The equivalent soil is modelled with the ‘Mohr-Coulomb’ law (Table 4). The stiffness of the equivalent soil is proportional to the replacement rate:

$$E_{eq} = \frac{E_{col} \cdot A_{col} + E_{soil} \cdot (A_{imp} - A_{col})}{A_{imp}} \quad (11)$$

Where E_{eq} , E_{col} and E_{soil} (kPa) are respectively the Young moduli of the equivalent soil, the stone column and the surrounding soil, and A_{col} and A_{imp} (m²) are respectively the plane section of the column and the ground surface improved by that column. For a triangular mesh, the surface improved by a stone column is given by:

$$A_{imp} = \frac{\pi}{4} \cdot d_{eq}^2 \approx \frac{\pi}{4} \cdot (1.05 \cdot s)^2 \quad (12)$$

Where d_{eq} (m) is the equivalent diameter of the improved area and s (m) is the axis-to-axis distance between the columns.

In a non-cohesive soil, the equivalent friction angle is determined similarly:

$$\tan \phi'_{eq} = \frac{\tan \phi'_{col} \cdot A_{col} + \tan \phi'_{soil} \cdot (A_{imp} - A_{col})}{A_{imp}} \quad (13)$$

Where ϕ'_{col} and ϕ'_{soil} are respectively the effective friction angles of the stone column and of the surrounding soil.

6.4.2 Numerical approach

The characteristics of the equivalent soil are determined through numerical analyses, in oedometric or triaxial conditions for few columns explicitly modelled; load/deformations curves provide with ‘Hardening soil’ type parameters.

The positive effect of stone columns on the enclosing soil is partly due to compaction during the installation of the stone column. Calculating this

effect is time-consuming. A turnaround is found by playing with the overconsolidation ratio (OCR) in the surrounding soil, changing the apparent soil stiffness. OCR is here a calculation parameter whose exact value is by nature unknown.

It is hence relevant considering the sensitivity of the results to this parameter. Too large OCR values should be avoided ($OCR \leq 1.5$).

The parameters considered in the auxiliary models are summarised in Table 5.

Table 2. Design parameters – bedrock (HSSmall)

Layer	Density		Shear strength		
	γ_{unsat} (kN/m ³)	γ_{sat} (kN/m ³)	c' (kPa)	φ' (°)	Ψ (°)
Bedrock – sound	19	20	100	50	0
Bedrock – weathered	19	20	100	50	0

Layer	Reference stiffness						
	E_{50}^{ref} (MPa)	E_{oed}^{ref} (MPa)	E_{ur}^{ref} (MPa)	m (-)	$\gamma_{0.7}$ (-)	G_0^{ref} (MPa)	OCR (-)
Bedrock – sound	85.4	42.7	427	1.0	1.7e-5	1770	1.0
Bedrock – weathered	70.6	35.3	353	1.0	4e-5	1240	1.0

Table 3. Design parameters – soft soils (Mohr-Coulomb)

Layer	Density		Shear strength		
	γ_{unsat} (kN/m ³)	γ_{sat} (kN/m ³)	c' (kPa)	φ' (°)	Ψ (°)
Silty/clayey alluvions (NW)	17	19	20	20	0
Silty/clayey alluvions (SE)	17	19	20	20	0
Gravelly alluvions	16	18	0	30	0

Layer	Reference stiffness		
	E_{Young} (MPa)	E_{oed} (MPa)	ν (-)
Silty/clayey alluvions (NW)	7.4	10	0.3
Silty/clayey alluvions (SE)	17.8	24	0.3
Gravelly alluvions	89.2	120	0.3

Table 4. Design parameters – improved soil (Mohr-Coulomb)

Layer	Density		Shear strength		
	γ_{unsat} (kN/m ³)	γ_{sat} (kN/m ³)	c' (kPa)	φ' (°)	Ψ (°)
Improved soil (NW)	19	19	20	25	0

Layer	Reference stiffness		
	E_{Young} (MPa)	E_{oed} (MPa)	ν (-)
Improved soil (NW)	18.6	25	0.3

Table 5. Design parameters – auxiliary models (HSSmall)

Layer	Density		Shear strength		
	γ_{unsat} (kN/m ³)	γ_{sat} (kN/m ³)	c' (kPa)	φ' (°)	Ψ (°)
Silty/clayey alluvions (NW)	17	19	20	20	0
Silty/clayey alluvions (SE)	17	19	20	20	0
Column gravel	19	19	0	45	0

Layer	Reference stiffness						
	E_{50}^{ref} (MPa)	E_{oed}^{ref} (MPa)	E_{ur}^{ref} (MPa)	m (-)	$\gamma_{0.7}$ (-)	G_0^{ref} (MPa)	OCR (-)
Silty/clayey alluvions (NW)	17.4	11.6	69.6	0.7	2.2e-4	79.2	≤1.5
Silty/clayey alluvions (SE)	41.9	27.9	167.4	0.7	1.5e-4	114.5	≤1.5
Column gravel	99.2	99.2	297.6	0.5	4.6e-5	255.3	1.0

7 FE MODELS

7.1 Auxiliary models

7.1.1 Triaxial conditions

A cylindric model contains a single column and the soil it influences (Figure 6a). The bottom is fully blocked. Normal distributed loads are applied to the top and on the side. Three isotropic consolidation pressures are applied (100, 200 & 400 kPa), then a shearing stage runs until failure is reached, defining the secant modulus E_{50}^{ref} and the shear strength.

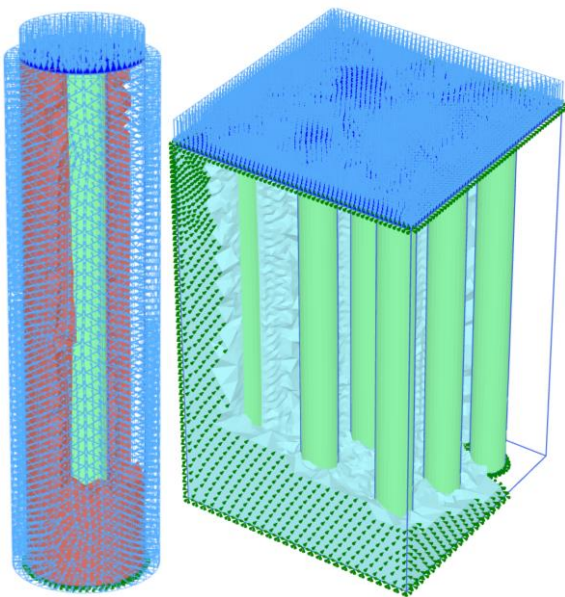


Figure 6 – Auxiliary models – triaxial and oedometric conditions (surrounding soil is partly hidden)

7.1.2 Oedometric conditions

Nine columns are modelled (Figure 6b). Triangular mesh is approximated to square-mesh to respect symmetry conditions at boundaries. A uniform distributed load is applied at the top of the model above a rigid plate. All displacements are blocked at the bottom of the model; normal displacements are blocked on the lateral boundaries. The model is loaded to 250 kPa, unloaded down to 50 kPa and reloaded to 1,000 kPa.

The results are analysed as an oedometric curve, determining the oedometer modulus E_{oed}^{ref} , the soil-type parameter m , and the ratio between primary and unloading/reloading moduli.

7.2 Global model

The present paper is not focussed on the global model, which is therefore briefly described.

The building is modelled by its walls (plate elements) and slabs (plate and volume elements). The model dimensions are 200x150x34 m³ (Length x width x height).

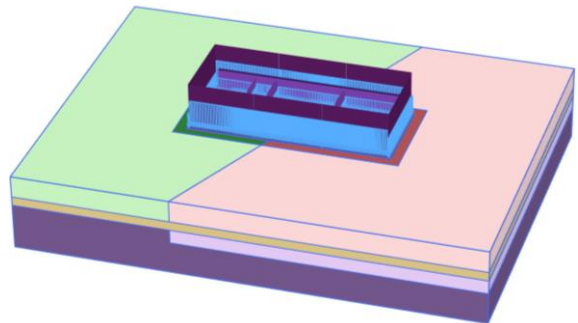


Figure 7 – Global model – the improved soil area shows darker colours than the unimproved area

8 RESULTS

8.1 Auxiliary models

Figure 8 and Figure 9 show the computed triaxial and oedometric curves for the composite soil. Figure 10 and Figure 11 show the curve fitting for the NW zone. The resulting parameters are presented in Table 6.

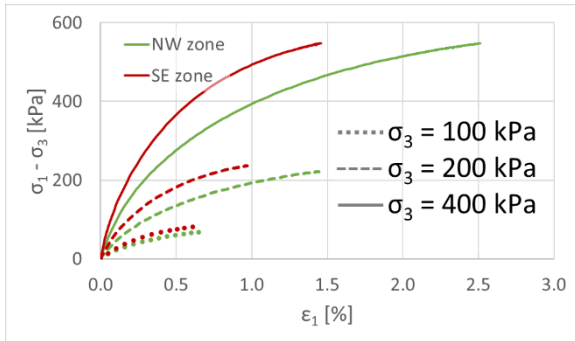


Figure 8 – Auxiliary model – triaxial conditions – vertical strain vs vertical deviatoric stresses

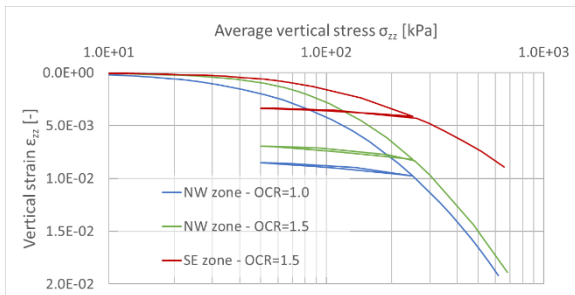


Figure 9 – Auxiliary model – oedometric conditions – vertical strain vs vertical stresses

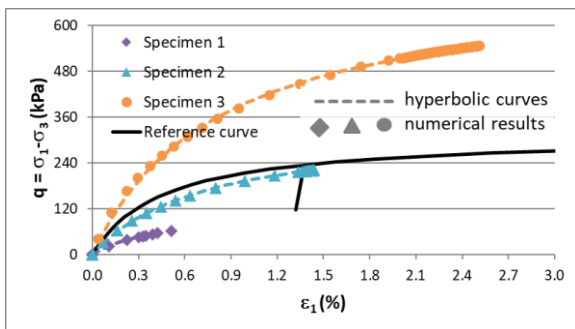


Figure 10 – NW zone – triaxial conditions – theoretical (hyperbolic) curves vs numerical results – the

reference curve is the theoretical one for the reference stress of 100 kPa

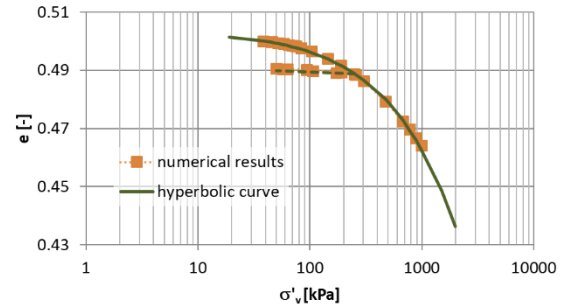


Figure 11 – NW zone – oedometric conditions – theoretical (hyperbolic) curves vs numerical results (OCR = 1.5)

8.2 Global model

The settlements computed with the global model, using the parameters determined with either the empirical approach or the numerical approach are summarised in Table 7. The numerical approach provides with a significant decrease of the computed settlements.

9 RESULTS VALIDATION

In order to validate the design, a large-scale loading test has to be performed on a limited number of preproduction stone columns installed at the site. Soil displacements must be recorded during the loading test, and soil parameters must also be surveyed before and after the installation of the stone columns.

A back-analysis of the loading test must be performed, based on the local soil parameters. Playing with the soil parameters in the auxiliary models will provide with updated equivalent parameters able to reproduce the loading test; the global model will therefore be updated and the design will be either validated or adapted to comply with the imposed settlement criteria.

10 CONCLUSIONS

The use of auxiliary FE-models allows a finer determination of equivalent soil parameters for stone-column improved soils. Although the obtained parameters still need to be validated

through relevant testing, it is anticipated that the proposed method will provide with a more accurate prediction of the settlements of large structures than the usual empirical estimates.

Table 6. Improved soils – resulting parameters from auxiliary models (HSSmall)

Layer	Density		Shear strength		
	γ_{unsat} (kN/m ³)	γ_{sat} (kN/m ³)	c' (kPa)	ϕ' (°)	Ψ (°)
Silty/clayey alluvions (NW – OCR = 1.0)	17	19	19.3	31	0
Silty/clayey alluvions (NW – OCR = 1.5)	17	19	19.3	31	0
Silty/clayey alluvions (SE – OCR = 1.5)	17	19	24.1	31.3	0

Layer	Reference stiffness						
	E_{50}^{ref} (MPa)	E_{oed}^{ref} (MPa)	E_{ur}^{ref} (MPa)	m (-)	$\gamma_{0.7}$ (-)	G_0^{ref} (MPa)	OCR (-)
Silty/clayey alluvions (NW – OCR = 1.0)	37.5	22	150	0.5	1e-4	150	1.0
Silty/clayey alluvions (NW – OCR = 1.5)	37.5	26	225	0.3	1e-4	225	1.5
Silty/clayey alluvions (SE – OCR = 1.5)	56	55	225	0.3	1e-4	225	1.5

$\gamma_{0.7}$ and G_0^{ref} are based on engineering judgment: $\gamma_{0.7} \approx 10^{-5} \dots 10^{-4}$ and $G_0^{ref} \approx E_{ur}^{ref}$ (Brinkgreve, 2014)

Table 7. Global model – Minimum and maximum computed settlements

Model layout			Settlements (mm) (deadloads)		Settlements (mm) (dead + live loads)	
Approach	SE zone?	OCR	Min	Max	Min	Max
Empirical	No	--	16	37	33	60
Numerical	No	1.0	5	24	20	45
Numerical	No	1.5	4	22	18	41
Numerical	Yes	1.5	3	19	16	33

11 REFERENCES

Lunne T, Robertson P.K. et Powell J.J.M, 1997, *Cone Penetration Testing in Geotechnical Practice*, Blackie Academic & Professional, London

Brinkgreve, R.B.J. 2014. The HS and HSSmall models and parameters, *Advanced course in computational geotechnics*, Plaxis BV, The Netherlands

Brinkgreve R et al, 2017, *Plaxis 3D 2017 User's manuals*, Plaxis BV, The Netherlands